

Investigation of Cryogenic Current-Voltage Anomalies in SiGe HBTs: Role of Base-Emitter Junction Inhomogeneities

Nachiket R. Naik, Bekari Gabritchidze, Jacob Kooi, Kieran A. Cleary, Austin J. Minnich

Abstract—The anomalous current-voltage characteristics of cryogenic SiGe heterojunction bipolar transistors (HBTs) have been a topic of investigation for many years. Proposed explanations include quasiballistic transport of electrons across the base or tunneling from the emitter to the collector, but inconsistencies exist with these hypotheses. Although similar behavior occurs in Schottky junctions and has been attributed to spatial inhomogeneities in the base-emitter junction potential, this explanation has not been considered for SiGe HBTs. Here, we experimentally investigate this hypothesis by characterizing the base-emitter junction ideality factor and built-in potential of a SiGe HBT versus temperature using a cryogenic probe station. The temperature-dependence of the ideality factor and the relation between the built-in potential as measured by capacitance-voltage and current-voltage characteristics are in good qualitative agreement with the predictions of a theory of electrical transport across a junction with a Gaussian distribution of potential barrier heights. These observations support the origin of cryogenic electrical anomalies in SiGe HBTs as arising from lateral inhomogeneities in the base-emitter junction potential. This work helps to identify the physical mechanisms limiting the cryogenic microwave noise performance of SiGe HBTs.

Index Terms—Heterojunction bipolar transistors, SiGe, cryogenic microwave amplifiers, device physics, barrier inhomogeneities, ideality factor, microwave noise.

I. INTRODUCTION

Silicon-germanium heterojunction bipolar transistors (HBTs) are widely used in microwave applications such as high-speed communications and radar systems owing to their competitive microwave performance, low cost, and ease of integration compared with III-V compound semiconductor devices [1]. Technological advances such as reduced emitter widths, decreased base resistances and extrinsic capacitances, and advanced epitaxial techniques have enabled RF performance rivaling that of III-V high electron mobility transistors [2], [3]. Recently, owing to these

strengths, cryogenic SiGe HBTs have been considered for applications in quantum computing and radio astronomy [4], [5].

The cryogenic microwave performance of SiGe HBTs has been investigated following their initial development in the 1980s [6] as various performance metrics such as transconductance and noise figure improve with cooling. However, below ~ 77 K, these improvements are observed to plateau with decreasing temperature [7], [8], corresponding to a temperature-dependent base-emitter junction ideality factor $n(T)$ that greatly exceeds unity at cryogenic temperatures [9], [10]. This behavior differs markedly from the predictions of drift-diffusion theory of an ideal p-n junction in which n is equal to unity and is independent of temperature, and the transconductance increases inversely with temperature. [11], [12] This cryogenic non-ideal behavior has been attributed to various mechanisms including quasiballistic transport [8], [13], direct tunneling [9], or trap-assisted tunneling [14]. However, a recent theory work has reported that quasiballistic electron transport cannot explain the observed collector cryogenic non-idealities [15]. Further, these non-idealities have been observed in devices with base widths of ~ 100 nm [5] for which direct tunneling is negligible. As a result, the origin of these cryogenic anomalies remains a topic of investigation.

In a different context, similar anomalies have been observed and extensively investigated in Schottky diodes [16], [17], [18], [19], and they were ultimately attributed to spatial inhomogeneities in the built-in potential Φ_{BI} . [20], [21], [22], [23] Although semiconductor junctions are often modeled as uniform across the lateral area, in fact various imperfections exist which affect the local electronic structure of the junction, a point which was recognized as early as 1950. [24] Even at epitaxial interfaces, it was found that different crystallographic orientations [25], [26], [27] or the presence of dislocations [28], [29] can lead to potential barrier height variations on the order of hundreds of mV. In Schottky junctions, these inhomogeneities have been directly observed using ballistic electron emission microscopy, which allows the local barrier height to be mapped with nanometer spatial resolution. [30], [31] Various theories and numerical analyses of the electrical characteristics of inhomogeneous junctions have been reported and lead to compatible conclusions. [22], [20], [21] For concreteness, the theory of Werner and Güttler assumes a Gaussian distribution of barrier heights and makes several predictions regarding the temperature-dependence of the ideality factor and the relation between the built-in potential as

Manuscript submitted on October 17, 2023.

This work was supported by NSF Award Number 1911926 and by JPL PDRDF Project Number 107978.

N. R. Naik is with the Division of Engineering and Applied Sciences, California Institute of Technology, Pasadena, CA 91125, USA (e-mail: nnaik@caltech.edu)

B. Gabritchidze is with the Cahill Radio Astronomy Lab, California Institute of Technology, Pasadena, CA 91125, USA

K. A. Cleary is with the Cahill Radio Astronomy Lab, California Institute of Technology, Pasadena, CA 91125, USA

J. Kooi is with NASA Jet Propulsion Laboratory, California Institute of Technology, Pasadena, CA 91109, USA

A. J. Minnich is with the Division of Engineering and Applied Sciences, California Institute of Technology, Pasadena, CA 91125, USA (e-mail: aminnich@caltech.edu).

measured by different methods. [21], [32], [33] However, an experimental test of these predictions for SiGe HBTs has not yet been reported.

Here, we perform this experimental investigation by characterizing the ideality factor and built-in potential of a SiGe HBT from room to cryogenic temperatures. We find that the measured temperature-dependence of the ideality factor and the relation between built-in potential as determined by capacitance-voltage and current-voltage characteristics are compatible with the theory. This observation supports the origin of the cryogenic electrical anomalies as arising from inhomogeneities in the base-emitter junction potential. We suggest a possible physical origin of the inhomogeneities as Ge clusters or electrically active C impurities which are introduced to minimize dopant diffusion, and we discuss how the existence of barrier inhomogeneities could be further confirmed and mitigated in optimized devices. Our work advances efforts to improve the cryogenic electrical characteristics and hence microwave noise performance of SiGe HBTs.

II. THEORY AND METHODS

A. Overview

The theory of Werner and Güttler describes electrical transport across a potential barrier with heights distributed according to a Gaussian distribution of a specified mean and variance. [21] The variance of the distribution is assumed to decrease with increasing junction bias due to the pinch-off of low-barrier patches of dimension less than the depletion length, a concept that was originally introduced in [22] and later developed in [20]. The theory makes several predictions regarding the trends of electrical characteristics with temperature and other parameters in junctions exhibiting voltage-independent ideality factors $n(T)$. In particular, $n(T)$, as determined from the slope of $I - V$ characteristics, is predicted to vary with temperature according to $n(T)^{-1} - 1 = -\rho_2 + \rho_3/(2kT/q)$ where k is Boltzmann's constant, q is the electric charge, and ρ_2 and ρ_3 are constants describing the variation of the mean and variance of the potential barrier distribution with junction voltage, respectively (see [21, Eq. 23]). A plot of $n(T)^{-1} - 1$ versus T^{-1} should therefore yield a line over some range of temperatures.

In addition, the built-in potential Φ_{BI} can be measured in two ways. From $C_{BE} - V_{BE}$ characteristics, $\Phi_{BI}(CV)$ can be obtained by fitting the variation of depletion capacitance with junction voltage using $C_{BE}(V_{BE}) = C_{BE,0}(1 - V_{BE}/\Phi_{BI})^{-m}$, where $C_{BE,0}$ is the zero-bias junction capacitance and m is an exponent that depends on the doping profile at the junction. [12] Using $I_C - V_{BE}$ characteristics, the potential barrier energy for transport, E_a , relative to its value at some temperature, can be obtained by extrapolating the measured collector current to zero bias using the collector current expression $I_C = I_S(\exp(qV_{BE}/n(T)kT) - 1)$ where $I_S = A \exp(-qE_a/kT)$ is the transport saturation current and A is a constant prefactor. [1, Sec. 4.2.1] With the value of the transport barrier at 300 K specified as $\Phi_{BI}(CV)$, the temperature-dependence of the apparent built-in potential associated with charge transport $\Phi_{BI}(IV)$ can thus be obtained from change in I_S at each temperature compared to

the value at the reference temperature. The theory predicts that the barrier measured in these two ways should differ in magnitude and temperature dependence owing to the fact that current depends on V_{BE} exponentially while the capacitance varies with V_{BE} with a weaker polynomial dependence. The barrier as determined through $C - V$ characteristics is therefore typically interpreted as the mean barrier height, while that determined from $I - V$ characteristics is often less than the mean value due to the larger contribution from low-barrier regions. [34], [21] The theory gives a relation between these barrier heights. [21, Eq. 14] Considering the form of $n(T)$ described above, this relation is compatible with the empirical observation that $\Phi_{BI}(CV) \approx n(T)\Phi_{BI}(IV)$ [35] (see also [21, Sec. V]).

These predictions can be tested using a cryogenic probe station to measure the $I_C - V_{BE}$ and $C_{BE} - V_{BE}$ characteristics of a SiGe HBT. We note that for the $C_{BE} - V_{BE}$ characteristics, although the mechanisms of current transport in the forward active regime differ between Schottky junctions and HBTs, the electrostatics of the depletion capacitance are identical between the devices. [36, Chaps. 6 and 7] Therefore, the built-in potential can be determined by the dependence of C_{BE} on V_{BE} for biases for which C_{BE} is dominated by the depletion capacitance. This procedure was applied to determine the built-in potential of SiGe HBTs in another study. [10]

B. Experimental methods

We extracted Φ_{BI} from $C_{BE} - V_{BE}$ and $I_C - V_{BE}$ characteristics from 20 – 300 K on a SiGe HBT (SG13G2, IHP). The discrete transistors were probed in a custom-built cryogenic probe station. [37], [38] We employed Nickel/Tungsten probes (40A-GSG-100-DP, GGB Industries) which are suitable for probing Al pads. $I_C - V_{BE}$ characteristics were performed at a constant collector voltage $V_{CE} = 1$ V to provide a collector current above the minimum resolution of our measurement setup (10 nA). The current range used for this fitting is limited to 0.2 mA, below the high-injection regime, to exclude effects of series resistance, self-heating and the Early and reverse Early effects. Inclusion of the reverse Early effect in the extraction of the built-in potential was found to alter the value by only a few percent. The low-injection regime below $\sim 1 \mu\text{A}$ was also excluded from the fitting to ensure that the current corresponded to charge injection over the base-emitter potential barrier. Φ_{BI} was extracted relative to its value determined by $C_{BE} - V_{BE}$ measurements at 300 K from the zero-bias intercept of a linear fit of $\ln(I_C)$ versus V_{BE} , and $n(T)$ was extracted from the slope of this fit.

Following standard procedure, [10], [11] $C_{BE} - V_{BE}$ characteristics were obtained using a vector network analyzer (VNA, Keysight E5061B). In reverse-bias and low-forward bias regimes, the Y -parameters are given by $Y_{11} = g_{BE} + j\omega(C_{BE} + C_{BC})$ and $Y_{12} = -j\omega C_{BC}$, where C_{BC} is the base-collector depletion capacitance. The base-emitter capacitance can therefore be expressed as $C_{BE} = (\Im(Y_{11} + Y_{12}))/2\pi f$. V_{BE} was restricted to $[-0.5 \text{ V}, +0.5 \text{ V}]$ to ensure that the measured capacitance was dominated by the depletion

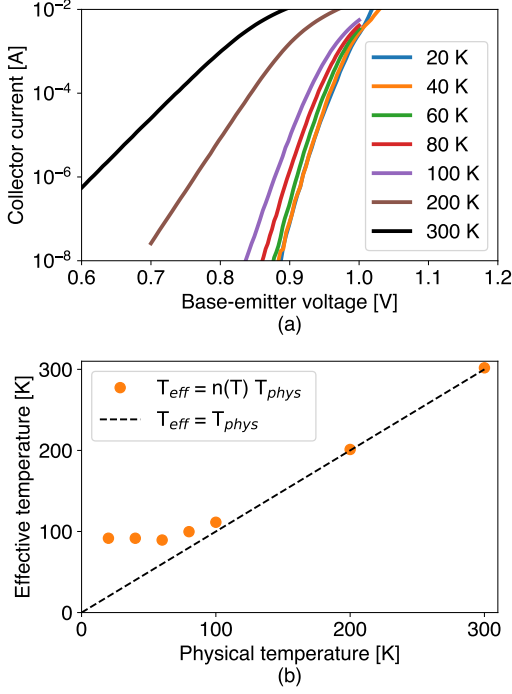


Fig. 1 (a) Measured I_C versus V_{BE} for various temperatures. The characteristics become independent of temperature at cryogenic temperatures. (b) $T_{eff} = n(T)T_{phys}$ vs T_{phys} from measurements (symbols) and diode theory (line), indicating the non-ideality of the base-emitter junction at cryogenic temperatures.

capacitance. $V_{BC} = 0$ V was held constant to ensure C_{BC} was constant while V_{BE} was swept. The Y parameters were measured in 1 – 3 GHz, and the extractions were performed at 2.4 GHz. At these frequencies, it was observed that the imaginary part of Y_{11} was linear in frequency, indicating purely capacitive behavior. Short-Open-Load-Through calibration was performed on a CS-5 calibration standard at each temperature, and the shunt parasitic capacitance at the input of the device was de-embedded using an OPEN structure. The intermediate-frequency bandwidth (1 kHz) and frequency points (every 0.2 GHz) were selected to limit the total sweep time to less than 15 s to avoid drift. At each bias, Y -parameters were swept across frequency and ensemble-averaged 10 times. Φ_{BI} was extracted from a sweep of C_{BE} versus V_{BE} by fitting the parameters Φ_{BI} , $C_{BE,0}$ and m using a trust region reflective algorithm from the SciPy library. [39] Φ_{BI} was constrained to [0.5 V, 1.2 V], $C_{BE,0}$ was constrained between the minimum and maximum values of the sweep, and m was constrained to [0, 1].

III. RESULTS

Fig. 1a shows the collector current I_C versus V_{BE} at various temperatures between 20 K and 300 K. Consistent with prior findings, [5], [8], [9] the measurements exhibit deviations with theory at cryogenic temperatures, with the current failing to follow the temperature trend expected from the diode equation below ~ 100 K. We plot the extracted $n(T)$ as $T_{eff} = n(T)T_{phys}$ versus T_{phys} in Fig. 1b. T_{eff} is

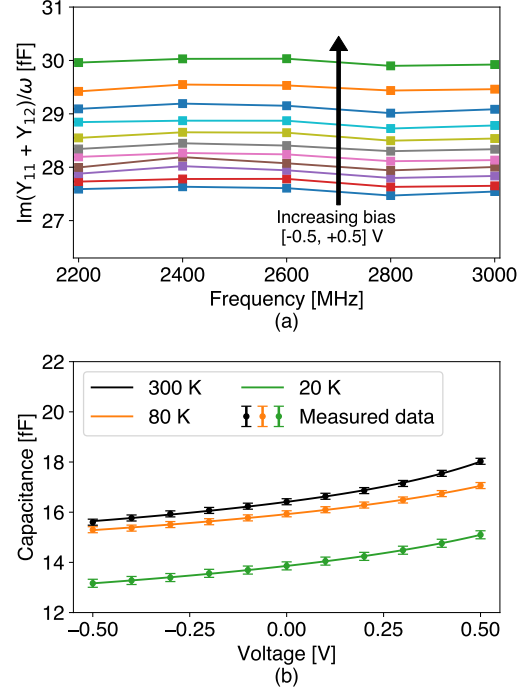


Fig. 2 (a) Measured $\Im(Y_{11} + Y_{12})/\omega$ (symbols) versus f at 300 K for various V_{BE} in steps of 0.1 V. The lines are guides to the eye. (b) Measured (symbols) and fitted (solid lines) C_{BE} versus V_{BE} at 300 K, 80 K and 20 K. As a representative example, the fit for 300 K yields $\Phi_{BI} = 0.83$ V and $m = 0.10$.

observed to plateau to ~ 100 K due to $n(T) > 1$ at cryogenic temperatures, as has been reported previously [8].

We next examine the RF characteristics. Fig. 2a plots $\Im(Y_{11} + Y_{12})/\omega$ versus f for various V_{BE} at 300 K, where $\omega = 2\pi f$. A narrowed frequency range from the 1 – 3 GHz measurements is plotted to aid in distinguishing the curves. The de-embedded base-emitter capacitance C_{BE} is directly obtained from this plot by averaging across the frequency range. Fig. 2b plots the resulting C_{BE} versus V_{BE} at three representative temperatures across the overall voltage range along with the fitted curves. The error bars, representing the 2σ error in C_{BE} , are obtained from the 10 $C_{BE} - V_{BE}$ sweeps performed at each temperature.

These data are next analyzed to obtain Φ_{BI} from the $I_C - V_{BE}$ and $C_{BE} - V_{BE}$ characteristics according to the procedures in Section II-B. At 300 K, $\Phi_{BI}(CV)$ is found to be 0.83 V, in good agreement with [10]. This value is specified as the room temperature value for $\Phi_{BI}(IV)$ to facilitate comparison at other temperatures. Fig. 3a plots the Φ_{BI} from both measurements versus T_{phys} . For $\Phi_{BI}(CV)$, the error bars represent the $2-\sigma$ error in Φ_{BI} , obtained by performing fits to 100 $C_{BE} - V_{BE}$ sweeps with errors randomly determined based on a normal distribution defined by the uncertainty in the measured C_{BE} . The extracted $\Phi_{BI}(CV)$ is observed to weakly increase with decreasing temperature, consistent with observations for similar HBT devices [10] and Schottky diodes [35]. In contrast, $\Phi_{BI}(IV)$ exhibits a qualitatively stronger dependence on temperature than $\Phi_{BI}(CV)$

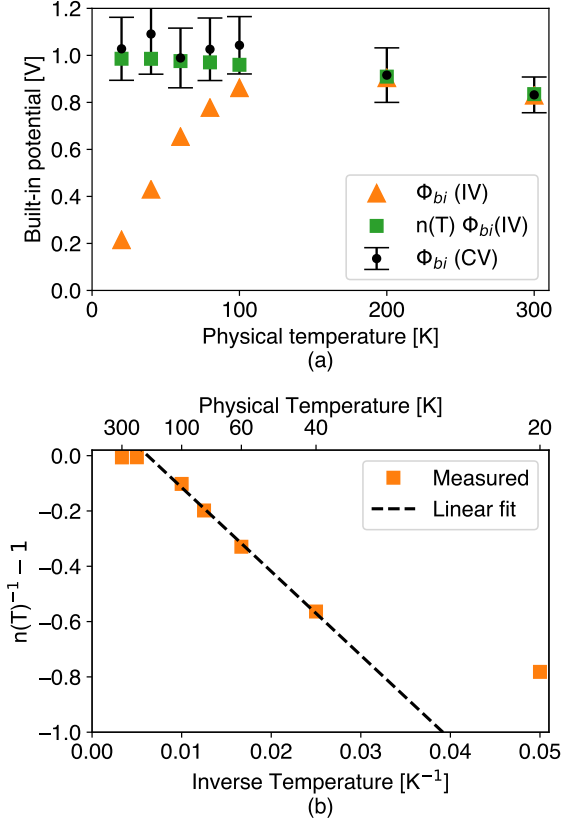


Fig. 3 (a) Built-in potential Φ_{BI} versus physical temperature from $C_{BE} - V_{BE}$ (black circles) and $I_C - V_{BE}$ (orange triangles) measurements. Also plotted is $n(T)\Phi_{BI}(IV)$ (green squares) which is predicted to agree with $\Phi_{BI}(CV)$. [21] Good agreement is observed. (b) $n(T)^{-1} - 1$ versus inverse physical temperature T^{-1} for measured data along with a linear fit to the data in 40-100 K following the prediction in [21].

and differs markedly in magnitude at cryogenic temperatures, as observed previously for Schottky diodes [35], [11] (also compare to [32, Fig. 3]). The variation with temperature of $\Phi_{BI}(IV)$ is significantly stronger than that of the emitter and base band gaps, [12] suggesting another mechanism is responsible for the observed temperature trend.

We now examine the agreement between the data and the predictions from the inhomogeneous junction theory of [21]. First, qualitatively, $\Phi_{BI}(CV)$ and $\Phi_{BI}(IV)$ are predicted to differ, with $\Phi_{BI}(IV)$ expected to exhibit a stronger temperature dependence and be smaller in magnitude than $\Phi_{BI}(CV)$. This behavior is observed in Fig. 3a. More quantitatively, for the predicted temperature-dependence of $n(T)$ from the theory, it is expected that $\Phi_{BI}(CV) \approx n(T)\Phi_{BI}(IV)$ [21, Sec. V]. The product $n(T)\Phi_{BI}(IV)$ is also plotted in Fig. 3a, demonstrating good agreement with $\Phi_{BI}(CV)$. Second, [21, Eq. 23] predicts that $n(T)^{-1} - 1$ versus T^{-1} should be a straight line over some range of temperatures. Fig. 3b plots this quantity, showing that the expected trend is observed over a temperature range which is comparable in relative width to

that in [21, Fig. 9]. Deviations at the lowest temperatures are noted, which may arise from the assumption of temperature-independent barrier properties in the original theory. Other explanations for stronger temperature dependencies compared to that predicted at this level of theory have been proposed in terms of the breadth of the distribution of barrier heights. [20] However, overall the experimental trends are in good qualitative agreement with the theoretical predictions.

Semi-quantitative information regarding the variation of the barrier height variance with bias can be obtained from the linear fit in Fig. 3b. If $\rho_2 + \rho_3 / (2kT/q) \ll 1$, the theory of [21] reduces to the T_0 model for non-ideal junctions that has been extensively studied in the Schottky junction literature. [17], [20], [21] In this case, the slope of the linear fit in Fig. 3b is simply T_0 . Performing this fit for the present data yields $T_0 \approx 30$ K, a value which is generally compatible with values for Schottky diodes compiled in [21]. Using [21, Eq. 33], this value can be recast in terms of the narrowing of the potential barrier height distribution with increasing bias using $\rho_3 \approx -2kT_0/q$. We obtain a value $\rho_3 = -5.2$ mV. The magnitude of this value indicates that changes in standard deviation of the potential barrier height distribution with base-emitter bias which are less than a percent of the mean barrier height are sufficient to account for the observed electrical anomalies.

IV. DISCUSSION

The agreement of our data with the predictions of the inhomogeneous barrier theory provides evidence that lateral inhomogeneities in the base-emitter junction potential are the origin of the cryogenic electrical anomalies. However, we note that other mechanisms such as electron tunneling [5], [9], conduction band tail effects [40], and junction periphery effects may still play a role in the electrical anomalies, and further study is necessary to test these other possibilities. Additional evidence for the barrier inhomogeneity hypothesis could be obtained using techniques such as ballistic emission electron microscopy which directly measure the spatial profile of the built-in potential. [31] However, applying this method to SiGe HBTs would require specialized samples to be prepared which are compatible with the measurement technique.

The materials-scale origin of the inhomogeneities in HBTs could be Ge clusters [41] or electrically active carbon defects [42]. Non-uniform Ge content over a few nanometers in SiGe p-wells with Ge concentration $\geq 30\%$ has been reported to lead to the degradation of electrical properties like hole mobility. [41] Trap states associated with C impurities have also been detected in modern HBTs. [42] With Ge concentrations for modern HBTs being on the order of 30% [9] and C doping on the order of 10^{20} cm^{-3} , [1] these defects could be responsible for spatial potential inhomogeneities at the base-emitter junction. If the presence of spatial inhomogeneities across the emitter area is verified, a less aggressive Ge doping concentration and profile, especially in narrow-base SiGe HBTs, could decrease the concentration of these imperfections and thereby lead to a more uniform base-emitter junction potential. The impact of structural properties on the electrical properties can be characterized by correlating

atomic-structural and electrical characterizations of SiGe heterojunction structures with varying Ge profiles.

Finally, we discuss the possible improvements in low-noise amplifier performance that may be obtained with more ideal base-emitter junctions. A more uniform base-emitter junction potential will result in cryogenic transconductance and collector current values which are closer to their ideal values. Improved ideality in these DC parameters directly affects the minimum noise temperature T_{min} of HBTs. For example, a decrease in T_{eff} from 80 K to the physical temperature 20 K, corresponding to an ideality factor at 20 K of $n = 1$ instead of $n = 4$, linearly improves the achievable T_{min} by a factor of 4 in the low-frequency and low base-resistance limit (see [4, Eq. 2]). Therefore, decreasing inhomogeneities in the base-emitter junction potential is expected to lead to improved cryogenic microwave noise performance, advancing their use in scientific and industrial applications.

V. CONCLUSION

We have reported a characterization of the base-emitter junction ideality factor and built-in potential versus temperature of a SiGe HBT. The observed trends with temperature and between measurement techniques agree with a theory of electrical transport at a potential barrier with a Gaussian distribution of barrier heights. The physical origin of these barrier inhomogeneities is hypothesized to be Ge clusters or C impurities. This work advances efforts to improve the cryogenic microwave noise performance of SiGe HBTs.

ACKNOWLEDGMENTS

The authors thank Sander Weinreb, Pekka Kangaslahti, Akim Babenko, Holger Rucker, Nicolas Derrier, John Cressler, and Xiaodi Jin for useful discussions. This work was supported by NSF Award Number 1911926 and by JPL PDRDF Project Number 107978.

AUTHOR DECLARATIONS

Conflict of Interest

The authors have no conflicts to disclose.

DATA AVAILABILITY

The data that support the findings of this study are available from the corresponding author upon reasonable request.

REFERENCES

- [1] J. D. Cressler and G. Niu, *Silicon-germanium heterojunction bipolar transistors*. Artech house, 2003.
- [2] P. Chevalier, M. Schroter, C. R. Bolognesi, V. D'Alessandro, M. Alexandrova, J. Bock, R. Flickiger, S. Fregonese, B. Heinemann, C. Jungemann, R. Lovblom, C. Maneux, O. Ostinelli, A. Pawlak, N. Rinaldi, H. Rucker, G. Wedel, and T. Zimmer, "Si/SiGe:C and InP/GaAsSb Heterojunction Bipolar Transistors for THz Applications," *Proceedings of the IEEE*, vol. 105, no. 6, pp. 1035–1050, 2017.
- [3] W. T. Wong, M. Hosseini, H. Rucker, and J. C. Bardin, "A 1 mW cryogenic LNA exploiting optimized SiGe HBTs to achieve an average noise temperature of 3.2 K from 4–8 GHz," in *2020 IEEE/MTT-S International Microwave Symposium (IMS)*. IEEE, 2020, pp. 181–184.
- [4] J. C. Bardin, S. Montazeri, and S. W. Chang, "Silicon germanium cryogenic low noise amplifiers," in *Journal of Physics: Conference Series*, vol. 834, no. 1. IOP Publishing, 2017, p. 012007.
- [5] H. Ying, J. Dark, A. P. Omprakash, B. R. Wier, L. Ge, U. Raghunathan, N. E. Lourenco, Z. E. Fleetwood, M. Mourigal, D. Davidovic, and J. D. Cressler, "Collector Transport in SiGe HBTs Operating at Cryogenic Temperatures," *IEEE Transactions on Electron Devices*, vol. 65, no. 9, pp. 3697–3703, 2018.
- [6] G. L. Patton, S. S. Iyer, S. L. Delage, S. Tiwari, and J. M. Stork, "Silicon-Germanium-Base Heterojunction Bipolar Transistors By Molecular Beam Epitaxy," *IEEE Electron Device Letters*, vol. 9, no. 4, pp. 165–167, 1988.
- [7] A. J. Joseph, J. D. Cressler, and D. M. Richey, "Operation of SiGe Heterojunction Bipolar Transistors in the Liquid-Helium Temperature Regime," *IEEE Electron Device Letters*, vol. 16, no. 6, pp. 268–270, 1995.
- [8] J. C. Bardin, "Silicon-Germanium Heterojunction Bipolar Transistors For Extremely Low-Noise Applications," Ph.D. dissertation, California Institute of Technology, 2009.
- [9] H. Rucker, J. Korn, and J. Schmidt, "Operation of SiGe HBTs at cryogenic temperatures," *Proceedings of the IEEE Bipolar/BiCMOS Circuits and Technology Meeting*, pp. 17–20, 2017.
- [10] X. Jin, M. Muller, P. Sakalas, A. Mukherjee, Y. Zhang, and M. Schroter, "Advanced SiGe:C HBTs at Cryogenic Temperatures and Their Compact Modeling with Temperature Scaling," *IEEE Journal on Exploratory Solid-State Computational Devices and Circuits*, vol. 7, no. 2, pp. 175–183, 2021.
- [11] W. Mönch, *Semiconductor Surfaces and Interfaces*. Springer Berlin, Heidelberg, 2001.
- [12] S. M. Sze, Y. Li, and K. K. Ng, *Physics of semiconductor devices*. John Wiley & sons, 2021.
- [13] D. M. Richey, A. J. Joseph, J. D. Cressler, and R. C. Jaeger, "Evidence for non-equilibrium base transport in Si and SiGe bipolar transistors at cryogenic temperatures," *Solid-State Electronics*, vol. 39, no. 6, pp. 785–789, 1996.
- [14] D. Davidović, H. Ying, J. Dark, B. R. Wier, L. Ge, N. E. Lourenco, A. P. Omprakash, M. Mourigal, and J. D. Cressler, "Tunneling, current gain, and transconductance in silicon-germanium heterojunction bipolar transistors operating at millikelvin temperatures," *Physical Review Applied*, vol. 8, no. 2, pp. 1–15, 2017.
- [15] N. R. Naik and A. J. Minnich, "Quasiballistic electron transport in cryogenic SiGe HBTs studied using an exact, semi-analytic solution to the Boltzmann equation," *Journal of Applied Physics*, vol. 130, no. 17, p. 174504, nov 2021.
- [16] R. Hackam and P. Harrop, "Electrical Properties of Nickel-Low-Doped n-Type Gallium Arsenide Schottky-Barrier Diodes," *IEEE Transactions on Electron Devices*, vol. 19, no. 12, pp. 1231–1238, 1972.
- [17] F. A. Padovani and G. G. Sumner, "Experimental study of gold-gallium arsenide schottky barriers," *Journal of applied physics*, vol. 36, no. 12, pp. 3744–3747, dec 1965. [Online]. Available: <http://aip.scitation.org/doi/10.1063/1.1713940>
- [18] A. Saxena, "Forward current-voltage characteristics of schottky barriers on n-type silicon," *Surface science*, vol. 13, no. 1, pp. 151–171, jan 1969. [Online]. Available: <https://linkinghub.elsevier.com/retrieve/pii/0039602869902453>
- [19] S. Ashok, J. Borrego, and R. Gutmann, "Electrical characteristics of GaAs MIS schottky diodes," *Solid-state electronics*, vol. 22, no. 7, pp. 621–631, jul 1979. [Online]. Available: <https://linkinghub.elsevier.com/retrieve/pii/0038110179901357>
- [20] R. T. Tung, "Electron transport at metal-semiconductor interfaces: General theory," *Physical Review B*, vol. 45, no. 23, pp. 13 509–13 523, 1992.
- [21] J. H. Werner and H. H. Güttler, "Barrier inhomogeneities at Schottky contacts," *Journal of Applied Physics*, vol. 69, no. 3, pp. 1522–1533, 02 1991. [Online]. Available: <https://doi.org/10.1063/1.347243>
- [22] J. L. Freeouf, T. N. Jackson, S. E. Laux, and J. M. Woodall, "Effective barrier heights of mixed phase contacts: Size effects," *Applied physics letters*, vol. 40, no. 7, pp. 634–636, apr 1982. [Online]. Available: <https://pubs.aip.org/apl/article/40/7/634/47889/Effective-barrier-heights-of-mixed-phase-contacts>
- [23] Y. Song, R. Van Meirhaeghe, W. Laflère, and F. Cardon, "On the difference in apparent barrier height as obtained from capacitance-voltage and current-voltage-temperature measurements on al/p-InP schottky barriers," *Solid-state electronics*, vol. 29, no. 6, pp. 633–638, jun 1986. [Online]. Available: <https://linkinghub.elsevier.com/retrieve/pii/0038110186901450>
- [24] V. A. Johnson, R. N. Smith, and H. J. Yearian, "D.c. characteristics of silicon and germanium point contact crystal rectifiers. part II. the multicontact theory," *Journal of applied physics*, vol. 21, no. 4, pp. 283–

- 289, apr 1950. [Online]. Available: <https://pubs.aip.org/jap/article/21/4/283/159274/D-C-Characteristics-of-Silicon-and-Germanium-Point>
- [25] R. T. Tung, "Schottky-barrier formation at single-crystal metal-semiconductor interfaces," *Physical Review Letters*, vol. 52, no. 6, pp. 461–464, feb 1984. [Online]. Available: <https://link.aps.org/doi/10.1103/PhysRevLett.52.461>
 - [26] R. J. Hauenstein, T. E. Schlesinger, T. C. McGill, B. D. Hunt, and L. J. Schowalter, "Schottky barrier height measurements of epitaxial NiSi₂ on si," *Applied physics letters*, vol. 47, no. 8, pp. 853–855, oct 1985. [Online]. Available: <https://pubs.aip.org/apl/article/47/8/853/51219/Schottky-barrier-height-measurements-of-epitaxial>
 - [27] R. Tung, A. Levi, J. Sullivan, and F. Schrey, "Schottky-barrier inhomogeneity at epitaxial NiSi₂ interfaces on si(100)." *Physical Review Letters*, vol. 66, no. 1, pp. 72–75, jan 1991. [Online]. Available: <http://dx.doi.org/10.1103/PhysRevLett.66.72>
 - [28] H. v. Känel, T. Meyer, and M. Klemenc, "Ballistic-electron-emission microscopy on epitaxial silicides," *Japanese journal of applied physics*, vol. 37, no. 6S, p. 3800, jun 1998. [Online]. Available: <https://iopscience.iop.org/article/10.1143/JJAP.37.3800>
 - [29] H. von Känel and T. Meyer, "Spectroscopy on MBE-grown interfaces with high spatial resolution," *Thin solid films*, vol. 306, no. 2, pp. 214–219, sep 1997. [Online]. Available: <https://linkinghub.elsevier.com/retrieve/pii/S0040609097001843>
 - [30] W. Kaiser and L. Bell, "Direct investigation of subsurface interface electronic structure by ballistic-electron-emission microscopy." *Physical Review Letters*, vol. 60, no. 14, pp. 1406–1409, apr 1988. [Online]. Available: <http://dx.doi.org/10.1103/PhysRevLett.60.1406>
 - [31] M. Prietsch, "Ballistic-electron emission microscopy (beem): Studies of metal/semiconductor interfaces with nanometer resolution," *Physics Reports*, vol. 253, no. 4, pp. 163–233, 1995.
 - [32] J. H. Werner and H. H. Güttler, "Transport properties of inhomogeneous schottky contacts," *Physica Scripta*, vol. T39, pp. 258–264, jan 1991. [Online]. Available: <https://iopscience.iop.org/article/10.1088/0031-8949/1991/T39/039>
 - [33] U. Rau, H. H. Güttler, and J. H. Werner, "The ideality of spatially inhomogeneous schottky contacts," *MRS Proceedings*, vol. 260, p. 245, 1992. [Online]. Available: <http://link.springer.com/10.1557/PROC-260-245>
 - [34] I. Ohdomari, T. S. Kuan, and K. N. Tu, "Microstructure and schottky barrier height of iridium silicides formed on silicon," *Journal of applied physics*, vol. 50, no. 11, pp. 7020–7029, nov 1979. [Online]. Available: <https://pubs.aip.org/jap/article/50/11/7020/291392/Microstructure-and-Schottky-barrier-height-of>
 - [35] A. S. Bhuiyan, A. Martinez, and D. Esteve, "A new Richardson plot for non-ideal Schottky diodes," *Thin Solid Films*, vol. 161, pp. 93–100, 1988.
 - [36] J. del Alamo, *Integrated Microelectronic Devices: Physics and Modeling*, 1st ed. Pearson, 2017.
 - [37] B. Gabritchidze, K. Cleary, J. Kooi, I. Esho, A. C. Readhead, and A. J. Minnich, "Experimental characterization of temperature-dependent microwave noise of discrete HEMTs: Drain noise and real-space transfer," in *2022 IEEE/MTT-S International Microwave Symposium-IMS 2022*. IEEE, 2022, pp. 615–618.
 - [38] D. Russell, K. Cleary, and R. Reeves, "Cryogenic probe station for on-wafer characterization of electrical devices," *Review of Scientific Instruments*, vol. 83, no. 4, p. 044703, 2012.
 - [39] P. Virtanen, R. Gommers, T. E. Oliphant, M. Haberland, T. Reddy, D. Cournapeau, E. Burovski, P. Peterson, W. Weckesser, J. Bright, S. J. van der Walt, M. Brett, J. Wilson, K. J. Millman, N. Mayorov, A. R. J. Nelson, E. Jones, R. Kern, E. Larson, C. J. Carey, Í. Polat, Y. Feng, E. W. Moore, J. VanderPlas, D. Laxalde, J. Perktold, R. Cimrman, I. Henriksen, E. A. Quintero, C. R. Harris, A. M. Archibald, A. H. Ribeiro, F. Pedregosa, P. van Mulbregt, and SciPy 1.0 Contributors, "SciPy 1.0: Fundamental Algorithms for Scientific Computing in Python," *Nature Methods*, vol. 17, pp. 261–272, 2020.
 - [40] A. Beckers, F. Jazaeri, and C. Enz, "Theoretical limit of low temperature subthreshold swing in field-effect transistors," *IEEE Electron Device Letters*, vol. 41, no. 2, pp. 276–279, 2019.
 - [41] R. A. Kiehl, P. E. Batson, J. O. Chu, D. C. Edelstein, F. F. Fang, B. Laikhtman, D. R. Lombardi, W. T. Masselink, B. S. Meyerson, J. J. Nocera, A. H. Parsons, C. L. Stanis, and J. C. Tsang, "Electrical and physical properties of high-Ge-content Si/SiGe p-type quantum wells," *Physical Review B*, vol. 48, no. 16, pp. 11 946–11 959, oct 1993.
 - [42] J. Raoult, F. Pascal, C. Delseny, M. Marin, and M. J. Deen, "Impact of carbon concentration on 1f noise and random telegraph signal noise in SiGe:C heterojunction bipolar transistors," *Journal of Applied Physics*, vol. 103, no. 11, pp. 114 508 1–10, 2008.